JOURNAL OF CATALYSIS **134**, 47–57 (1992)

Sodium-Doped V_2O_5/TiO_2 Systems: An XRD, DTA, TG/DTG, IR, V–UV, TPR, and XANES Study

PILAR MALET,* ADELA MUÑOZ-PÁEZ,* CRISTINA MARTÍN,†
AND VICENTE RIVES†,[1]

*Departamento de Química Inorgánica, Facultad de Química, Universidad de Sevilla, Sevilla, Spain; and
†Departamento de Química Inorgánica, Facultad de Farmacia,
Universidad de Salamanca, Salamanca, Spain

Received April 16, 1991; revised August 27, 1991

Vanadia–titania samples doped with different amounts of sodium have been prepared by impregnation of titania (P-25) with aqueous solutions of ammonium vanadate and calcination at 770 K, and have been characterized by X-ray diffraction, differential thermal analysis, thermogravimetric analysis, Fourier Transform-infrared spectroscopy, visible–ultraviolet (diffuse reflectance) spectroscopy, temperature-programmed reduction, and X-ray absorption near-edge structure spectroscopy. The results obtained indicate that doping the vanadia–titania system with increasing amounts of sodium leads initially to formation of V–Na–O compounds with a Na/V ratio close to 0.5 that are reduced at a higher temperature than V_2O_5, formed in the absence of sodium. If the amount of sodium is increased up to 3%, formation of Na_3VO_4 has been found.

INTRODUCTION

Vanadium oxide-based catalysts are widely used for catalytic oxidation of hydrocarbons. However, to achieve good activity and selectivity levels, V_2O_5 should be dispersed on a support. From several studies, it has been shown that one of the most successful supports is titania, normally used in the form of anatase (*1*). The TiO_2–V_2O_5 is a classical example of support enhancement of the active phase, specially if the metal oxide is applied on the carrier as a monolayer (*2*).

This system has been the object of several studies employing X-ray absorption spectroscopies (XAS) (*3*, *4*). According to these studies, it is generally assumed that the vanadia layer structure exposes the (010) plane and V=O groups preferentially, because of the excellent match of the vanadia unit and the anatase structure. It has been proposed that on the (001) plane of anatase, vanadium exists as monovanadate VO_4^{n-} groups bonded to the surface in such a way that the vanadium ion occupies roughly a position which a titanium ion would occupy if the bulk structure continues.

On the other hand, the interaction between substrate and catalyst depends on the acid–base properties of the catalyst, and hence several authors have tried to modify these acid–base properties by incorporating different promoters, usually alkaline ions, that in several occasions, specially when Na^+ ions are added, can lead to the formation of bronzes (*5*). The decrease in the activity for oxidation of hydrocarbons observed in these cases has been attributed to the presence of these bronzes.

To confirm or reject such hypothesis, the first step is to obtain structural information of the system. This is straightforward when crystalline phases are formed. However, the systems that show the most interesting catalytic properties are those with very low percentage of the active phase, where no crystalline phases can be formed. For such systems, XAS can provide unique information, since

---

[1] To whom all correspondence should be addressed.

0021-9517/92 $3.00

they are sensitive to the short range order (*6*), both in the EXAFS (Extended X-ray absorption fine structure) and XANES (X-ray absorption near-edge structure) regions. Additionally, partially reduced species (V^{4+}) should be present in the case of the formation of bronzes, in order to keep the electroneutrality of the system, and Lytle *et al.* (*7*) have reported changes in the XANES region of the XAS spectra of the V-edge ascribed to changes in the oxidation state of vanadium. These partially reduced species (V^{4+}) stabilized at the surface of the oxide have been claimed to play an important role in several catalytic processes (*8*).

Taking into account the above mentioned facts, in the present paper we report on a study of the structure of Vanadium oxide phases in several Na–V_2O_5–TiO_2 systems with different sodium contents. To get a deeper knowledge of the geometrical structure of such systems we have employed several complementary physical characterization techniques. The formation of crystalline phases has been checked with the aid of X-ray diffraction, and the XANES region of the XAS spectra of V-edge has been analyzed in the amorphous systems. The information obtained from the study of the Temperature Programmed Reduction profiles has shed light into the oxidation state of the vanadium species existing in the system. In order to gain a picture of the genesis of the oxide from the starting material, the decomposition of the catalysts precursors has been followed by DTA/TG, and IR spectroscopy has informed about the formation of new V–O bonds, since it is a technique very sensitive to slight changes in force constants.

EXPERIMENTAL

Samples were obtained from TiO_2 (P-25 from Degussa, $S_{BET} \approx 50\ m^2g^{-1}$). After calcination overnight at 770 K to withdraw adsorbed organic impurities, the support was doped with sodium (0, 0.5, 1 or 3% w/w) by impregnation with aqueous solutions of NaOH, while nitrogen was being continuously bubbled through the solution to avoid carbonate formation. The solvent was then eliminated by gentle warming at 353 K and the solid finally calcined at 773 K in oxygen. Incorporation of vanadia was performed by impregnating the Na-doped support with aqueous solutions of NH_4VO_3 (from Panreac) containing a small amount of oxalic acid (pH = 2) to make easier the solution of the salt. In all cases, the amounts of solution and support were chosen to yield after calcination final solids with 4.1% of vanadium (w/w), equivalent to the formation of a monolayer of vanadia, as determined from the specific surface area of the support and the area covered by a "molecule" of $VO_{2.5}$, $10.3 \times 10^4\ pm^2$ (*9*). The solvent was eliminated at 353 K, dried overnight at 383 K, and finally calcined in oxygen at 773 K. All calcination processes were performed at a heating rate of 10 K/min up to 773 K, this temperature being maintained for 3 h. Samples are designated as V-*X*, where *X* stands for the weight percentage of sodium.

X-ray diffraction (XRD) analysis was performed in a Philips PW 1070 instrument, using Ni-filtered Cu$K\alpha_1$ radiation (λ = 154.05 pm) and standard recording conditions. *Thermal analyses* of the solids obtained before calcination to decompose the precursor salt and to yield vanadia were carried out in Perkin–Elmer DTA-1700 and Perkin–Elmer TGS-2 instruments coupled to a Perkin–Elmer 3600 data station, in static air and with a heating rate of 10 K/min. *Infrared* spectra (IR) were recorded in a Perkin–Elmer FT-IR 1730 spectrometer, using KBr discs, with a nominal resolution of 4 cm^{-1} and averaging 100 spectra. A KBr disc with the same weight of the unloaded support was used to record the background spectrum in order to cancel all absorption bands due to the support. *Visible–Ultraviolet* spectra were recorded by the diffuse reflectance technique (V–UV/DR), in a Shimadzu UV-240 double beam spectrophotometer, with a slit of 5 nm and using MgO or parent TiO_2 as the reference. *Temperature programmed reduction* (TPR) were recorded in a conventional apparatus, with a catharometric detector, using a 5% H_2/Ar mixture as carrier gas, with a flow of 50 ml/min and a heating rate of 5 K/min. The amount of sample reduced (ca. 175 mg) corresponds to 140 μmol of V, thus ensuring good resolution under the experimental conditions employed (*10*). Deconvolution of the TPR profiles was performed by employing least square best-fit procedures with the aid of a FORTRAN 77 programme; the peaks are assumed pseudo-first-order (*10*), and the parameters being adjusted were height of the peak, position of the maximum, and half-width at half-height. *X-ray absorption* measurements of the supported vanadium catalysts were performed at the EXAFS station 8.1 of the SRS at Daresbury (UK). This station is operating with a double crystal monochromator Si(111) which was detuned 20% intensity to minimize the presence of higher harmonics. The resolution was estimated to be about 1 eV at the V *K*-edge (5464 eV) by a well-defined small peak in the main edge jump of a vanadium foil. The measurements were carried out in transmission using optimized ion chambers as detectors. Each data point was collected for 0.75 s and at least 4 scans were averaged, thus minimizing high and low frequency noise. Samples were pressed into thin-self supporting waffers using BN when necessary with an absorbance of ca. 2.5, and measured at room temperature. Standard procedures were used to extract the XANES data from the measured absorption spectra. Normalization was done by dividing by the height of the absorption edge, and the background was subtracted by using cubic spline routines.

RESULTS AND DISCUSSION

X-ray Diffraction

X-ray diffraction profiles of the samples are shown in Fig. 1. The profiles of samples V-0, V-0.5, and V-1 were identical to that of the bare support, differences being only detected in the XRD profile of sample V-3. In no case, peaks due to ternary Ti–V–O or Ti–Na–O compounds were detected, and peaks due to V_2O_5 (main peak at 438 pm) are also absent. The small peak close to 267 pm in the profile of sample V-3 can be ascribed to the presence of Na_4TiO_4, but this ascription should be discarded, as in the profile recorded for a sample containing the same amount of sodium, but without vanadium, and submitted to the same thermal treatment, it is recorded at a slightly lower spacing value. No peak has been recorded in any case that could be ascribed to Ti–V–O compounds (*11*). In all cases (support and vanadium-containing samples) the anatase content was 50% ± 5, as calculated from the intensities of the main diffraction peaks of rutile (110 planes) and anatase (101 planes), by applying the equation given by Criado and Real (*12*). So, the differences shown by our samples (see below) cannot be ascribed to a different interaction of vanadium compounds with anatase or rutile. The additional peaks recorded for sample V-3 can be ascribed to the presence of different, both stoichiometric and non-stoichiometric, ternary V–Na–O compounds. So, the peak close to 294 pm can be due to Na_3VO_4 (305 pm according to (*11*)), $Na_{0.33}V_2O_5$ (307 pm) or $Na_{1.33}V_2O_5$ (297 pm); that at 279 pm can be due to Na_3VO_4 (276 pm); and that at 267 pm also to Na_3VO_4 (267 pm). The peak recorded at 500 pm can be due to $NaVO_3$ (502 pm) or to $Na_{1.33}V_2O_5$ (498 pm), and it should be noted that a reflexion at 500 pm has been previously reported for non-stoichiometric Na–V bronzes ($Na_{1.33}V_2O_5$) in samples similar to those studied here (*5, 13*). So, this technique cannot be used to determine unambiguously the phases formed upon interaction of vanadium and sodium ions on the surface of titania, as the new XRD peaks recorded are not exclusive of a single compound.

Thermal Analyses

No special DTA or weight loss effects are to be expected for the calcined samples, but it is worth it to study the behaviour of the precursor solids (i.e., those obtained after impregnation and drying, but prior to calcination).

The TG/DTG and DTA profiles for the precursor of sample V-0 are shown in Fig. 2(a). Three steps can be seen from the TG

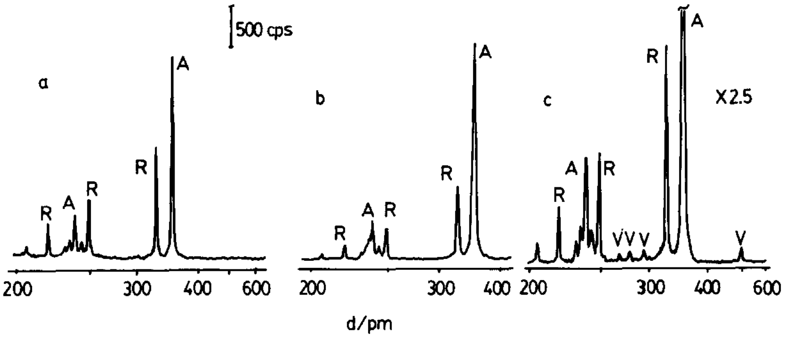

FIG. 1. X-ray diffraction profiles of (a) support and samples V-0 and V-0.5, (b) sample V-1, and (c) sample V-3. R = peaks due to rutile, A = peaks due to anatase, V = peaks due to vanadium compounds.

curve, better resolved through the DTG curve. According to these results, decomposition in air takes place through three overlapped steps (as no *plateau* is recorded in the TG curve), defined by the positions of the DTG peaks at 383, 493, and 613 K, with a more or less constant weight above this temperature. X-ray diffraction analysis of the residue after performing the TG study has revealed the presence of rutile, the high-temperature stable form of titania. Total weight loss was 14.35%. The DTA curve shows four effects: two endothermic ones, at 413 and 943 K, the last one due to vanadia melting (*5*), and two intense, exothermic effects at 525 and 623 K. The three low-temperature effects can undoubtedly be ascribed to the same processes giving rise to the weight loss effects recorded in the TG/DTG curve. Although vanadium has been incorporated from a solution of NH_4VO_3, addition of oxalic acid to favour solution of the vanadate salt gives rise to formation of the greenish-blue coordination compound, $[VO(C_2O_4)_2]^{2-}$ through reduction and coordination of V^{5+} ions (*14*).

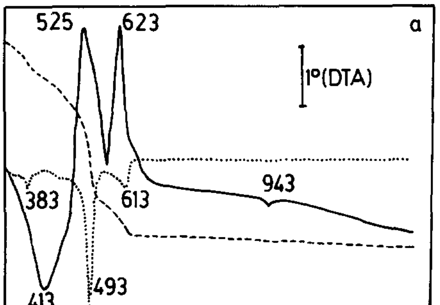

FIG. 2. Profiles from differential thermal analysis (solid line), thermogravimetric analysis (discontinuous line) and derivative thermogravimetric analysis (dotted line) of (a) sample V-0 and (b) sample V-3.

After drying at 383 K, a minor conversion to vanadia cannot be ignored, but the most part of the vanadium should have reacted with surface hydroxyl groups or be present as $(NH_4)_2[VO(C_2O_4)_2]$. With this, calcination to yield vanadia is not properly a decomposition of ammonium vanadate to vanadia, but decomposition and oxidation of the coordination compound, $[VO(C_2O_4)_2]^{2-}$, to vanadia. In addition, simple calculation of the weight loss recorded confirms such an assumption: Taking into account that final loading of vanadium is 4.1% (w/w) and ignoring the weight loss due to removal of surface hydroxyl groups (probably very much lower than the weight losses due to decomposition of the supported phase), the weight loss expected for decomposition of NH_4VO_3 to V_2O_5 would be 2.01%, smaller than the value experimentally recorded. However, the weight loss calculated for the process

$$(NH_4)_2[VO(C_2O_4)_2] \rightarrow V_2O_5$$

is 15.11%, in agreement, within experimental error, with the value experimentally obtained (14.35%). With that, the three main peaks recorded in the DTA diagram should be ascribed to different stages of decomposition of $(NH_4)_2[VO(C_2O_4)_2]$ that could mask removal of surface hydroxyl groups. Unfortunately, the nature of the gases evolved during decomposition could not be monitored.

The corresponding diagrams for sample V-3.0 in Fig. 2(b) are slightly different. Three minima are also recorded in the DTG profile, and their positions more or less coincide with those of sample V-0; the total weight loss recorded in this case was 12.5%, close to the expected value, but lower than that recorded for sample V-0. The shape of the DTA profile is also very similar, although in this case the effects are not so clearly defined, so indicating that the three stages take place more closely. The small endothermic effect at 943 K in the DTA profile of sample V-0 can be ascribed to melting of V_2O_5, already formed during the decomposition steps observed up to ca. 650 K. After calcination at 770 K vanadia should be poorly crystallized, as shown by the absence of diffraction peaks corresponding to this compound in the XRD profiles. This endothermic effect is not recorded for the V-3 sample, thus suggesting that part of the vanadia present in sample V-0 has reacted with Na^+ ions in sample V-3 to yield new compounds, in agreement with the XRD results.

It is worth noting that for both samples the only process detected above the calcination temperature is melting of vanadia, and therefore, additional chemical reactions between the supported phases and the TiO_2 support are not expected to happen when heating the samples up to 1150 K during the TPR experiments, in addition to reduction.

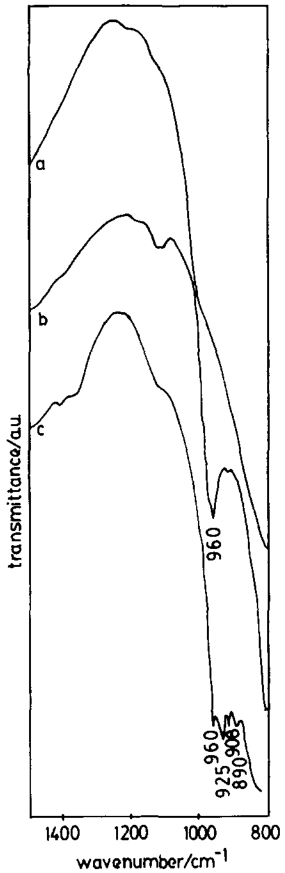

FIG. 3. FT-IR spectra of samples (a) V-0, (b) V-1, and (c) V-3.

Infrared Spectroscopy

The IR spectra of samples V-0, V-1 and V-3 are shown in Fig. 3. The spectrum for sample V-0.5 was almost identical to that recorded for sample V-0. The wavenumbers range shown in this Figure corresponds to the region where the absorption bands due to V–O stretching modes are expected, and their position and number have been related to different degree of crystallinity of the species containing them (*15*). For sample V-0, only a very weak shoulder can be recorded

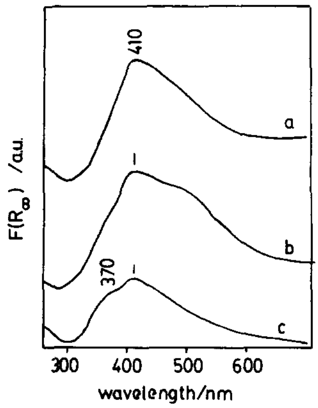

FIG. 4. Visible–Ultraviolet/Diffuse Reflectance spectra of samples (a) V-0, (b) V-1, and (c) V-3. Reference: unloaded TiO_2.

close to 1000 cm^{-1}, which has been ascribed (*15*) to poorly crystallized V_2O_5. Cancellation of the band at 1000 cm^{-1} has been found in samples of V_2O_5 supported on alumina when exposed to gaseous CO_2, indicating that surface carbonates are formed through reactions with exposed V=O species (*16*). For sample V-1 the band is now clearly recorded and is shifted to 960 cm^{-1}, and for sample V-3 a series of weak bands at 890, 908, 925, and 960 cm^{-1} are recorded. The peak at 1000 cm^{-1} has been reported to shift to 1025 cm^{-1} as the vanadia crystallinity increases (*15*), and so the lack of any band in this range of the spectrum of sample V-3 should be ascribed to the absence of crystalline V_2O_5 in this sample, in agreement with the XRD and DTA results above described. On the contrary, a set of bands close to 950 cm^{-1} has been reported by Bond *et al.* (*5*) in the IR spectra of vanadia supported on Na-doped anatase, and has been ascribed to formation of Na–V compounds.

Visible–Ultraviolet Spectroscopy

The V–UV/DR spectra of the samples in Fig. 4 show again differences when the sodium content is increased. All have been recorded *vs* parent titania, so the absorption band of this oxide below 400 nm, due to a $O^= \rightarrow Ti^{4+}$ charge transfer process (*17*) is cancelled. All three spectra are dominated by an absorption band close to 410 nm that is not an instrumental artifact due to a spurious cancellation of the named band of titania, as it is not recorded in the spectrum of a mechanical mixture of vanadia and titania recorded *vs* titania (*18, 19*). According to previous V–UV studies (*20*) performed with analogous samples, it has been concluded that this band at 410–420 nm should be ascribed to formation of peroxide-like species on the surface of titania, stabilized by the presence of vanadium ions. The absence of bands at 500 and 430 nm, due to $O^= \rightarrow V^{5+}$ charge transfer processes (*21*) in the spectra of samples V-O and V-3 again indicates the absence of crystalline V_2O_5 in these samples; however, this band can be recorded in the spectrum of sample V-1, indicating that some sintering of vanadium-containing species occurs in this sample. In addition, a shoulder at

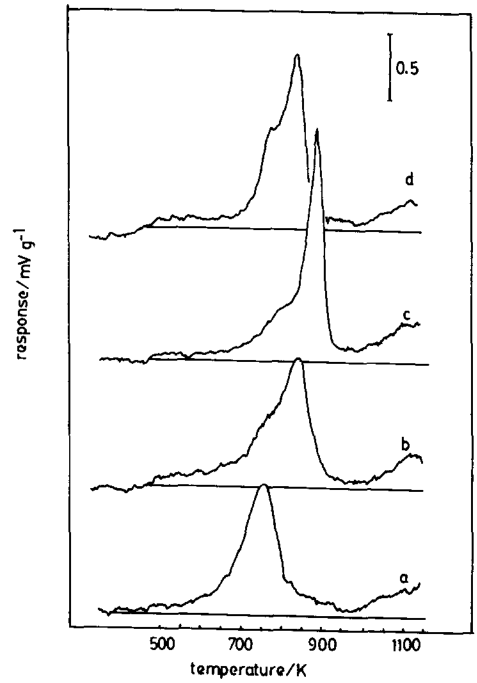

FIG. 5. Temperature Programmed Reduction profiles of samples (a) V-0, (b) V-0.5, (c) V-1, and (d) V-3.

TABLE 1

Results of the TPR Study of the Samples

Sample		V-0[a]	V-0.5	V-1.0	V-3.0
H_2 consumption/μmol (g catalyst)$^{-1}$					
470–970 K		935	918	939	954
470–1150 K		1155	1119	1243	1133
H_2/V ratio		1.43	1.39	1.55	1.41
	T_m/K	609	591	705	615
1	$\Delta T_{1/2}$/K	144	202	260	213
	μmol H_2/g	152	123	138	88
	T_m/K	753	755	804	781
2	$\Delta T_{1/2}$/K	99	101	90	80
	μmol H_2/g	623	211	180	305
	$\Sigma(1\text{–}2)$[b]	775	334	318	393
	T_m/K	823	841	895	846
3	$\Delta T_{1/2}$/K	50	84	60	56
	μmol H_2/g	46	468	508	466
	$\Sigma(1\text{–}3)$	821	802	826	859
	T_m/K	876	878	918	887
4	$\Delta T_{1/2}$/K	145	136	96	88
	μmol H_2/g	98	109	79	73
	$\Sigma(1\text{–}4)$	919	911	905	932
	T_m/K	1074	1074	1066	1074
5	$\Delta T_{1/2}$/K	184	155	152	231
	μmol H_2/g	18	7	25	17
	$\Sigma(1\text{–}5)$	937	918	930	949
μmol Na/g		0	217	435	1304

[a] Determination of H_2 consumption has been carried out from 370 K upwards for this sample.

[b] Accumulated H_2 consumption.

370 nm is recorded for sample V-3, although this band is also recorded in the spectrum of the support containing 3% Na, when recorded *vs* the pure, undoped support.

Temperature Programmed Reduction

The TPR profiles for all four samples containing vanadium are shown in Fig. 5. As the vanadium loading in all samples, 4.1% (w/w), is equivalent to 805 μmol V/g, the average hydrogen consumption up to 1150 K (1163 μmol/g, see Table 1) corresponds to ca. 1.5 hydrogen molecules per vanadium atom (1163/805 = 1.45); that is, reduction, under the experimental conditions here used and up to the maximum temperature here reached, leads to formation of V^{2+} species. Total hydrogen uptakes indicate that no major change exists in the oxidation state of vanadium in the calcined samples or in the whole reducibility up to 1150 K. Since previously reported XPS (*22–24*) and ESR (*25*) studies have shown that vanadium as V^{5+} species in undoped V_2O_5–TiO_2 catalysts calcined at 773 K, it should be concluded that V^{5+} species are also present in the calcined Na-doped samples, which reduce to V^{2+} at the maximum temperature reached here. In all cases, reduction takes place at temperatures below that needed to reduce bulk V_2O_5 under similar experimental conditions (reduction of these Na-containing samples starts at temperatures *ca.* 200–300 K lower than for bulk vanadia), and the degree of reduction is larger in these samples (H_2/V = 1.5 up to 1150 K) than in bulk vanadia (H_2/V = 1.0 up to 1250 K). The onset of the reduction process at a lower temperature for titania-supported as compared to that for unsupported vanadia has been ascribed (*26*) to the existence of a strong interaction between TiO_2 and the vanadium species, thus making its reduction easier. However, this decrease in reduction temperature has been also observed for well-dispersed vanadia supported on inert oxides (*27*) and should be better ascribed to a spreading of vanadia on the support and not to a particular interaction between vanadia and titania.

Reduction profiles show several maxima and have been submitted to a deconvolution analysis between 570–1170 K, keeping the number of components to the minimum needed to achieve a good fit between the experimental curve and the sum of the component bands. As an example, the results obtained for samples V-0 and V-3 are shown in Fig. 6. The positions of the maxima, hydrogen consumption (as calculated from the area under the curve after normalization) and width at half-height ($\Delta T_{1/2}$/K) are collected in Table 1. The different stages of reduction are numbered in this table according to the position (temperature) of the component bands.

Taking into account the total vanadium loading in the samples (805 μmol/g) and that in all four samples the reduction process leads to V^{2+} formation, three reduction steps are possible, according to

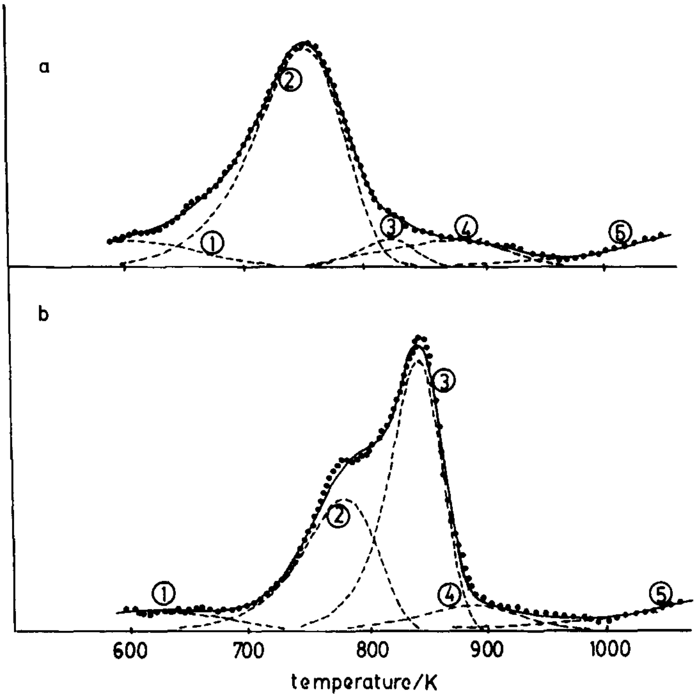

FIG. 6. Deconvolution analysis of the TPR profiles of samples (a) V-0 and (b) V-3.

$V^{5+} \rightarrow V^{4+}$ reaction (A)
$V^{4+} \rightarrow V^{3+}$ reaction (B)
$V^{3+} \rightarrow V^{2+}$ reaction (C).

The accumulated consumption of hydrogen for peaks [1] to [3] in all samples corresponds within 7% (see Table 1) to reduction of V^{5+} to V^{3+} (reactions (A) and (B)). Bands [4] and [5] in the TPR profiles would correspond to reaction (C), that starts at *ca.* 750–800 K and is not completed even at 1150 K. Step-by-step reduction of V^{5+} species to V^{3+}, as depicted by reactions (A) and (B) above, cannot be distinguished, as there is no combination of the hydrogen consumption amounts of components bands [1] to [3] that coincide with the amount of hydrogen required for the stoichiometric, V^{5+}/V^{4+} and V^{4+}/V^{3+} reductions. Then, it should be concluded that different surface V^{5+} species should exist, that are reduced to V^{3+} ones giving rise to the different first three TPR maxima.

The most significative differences among the behaviour shown by the samples here studied corresponds to these three first TPR maxima. In the absence of sodium, ca. 75% of the titania-supported vanadia reduces to V^{3+} in a single reduction process (peak 2) at 753 K (see Table 1 and Fig. 6). Less significative reduction processes are observed at lower (peak [1], 609 K) and higher temperatures (peak [2], 823 K), accounting respectively for 18 and 6% of the expected H_2 consumption for a complete reduction of V^{5+} to V^{3+}. As stated above, well-dispersed vanadia reduces at lower temperatures than the bulk oxide, and peaks [1] and [2] could be ascribed to such surface vanadia species, accounting for 94% of the vanadia present in the samples.

Addition of sodium (Fig. 5) shifts the TPR profile towards higher temperature. For the V-0.5 sample, deconvolution analysis (see Table 1) shows that peaks [1] (T_m = 609 K) and [2] (T_m = 755 K) are still present. Since their positions and widths at half-height coincide within experimental error with those observed in the undoped sample, these peaks are ascribed to supported vanadia that is not interacting with the sodium ions, accounting for 42% of the total vanadia present in the samples. Simultaneously, peak [3] at 841 K is now intense, accounting for reduction of 58% of the vanadia and indicating that a new type of surface vanadium species that must be interacting with sodium ions is now formed; the ratio between the amount of sodium existing in this sample and the amount of vanadium species reacted in this process is 217/468 = 0.46; in other words, in this new species existing in sample V-0.5 where vanadium is interacting with the added sodium ions, the Na/V ratio should be close to 0.46.

Band [2] is also observed for sample V-3, although it is narrower and is slightly shifted (*ca.* 25 K) to a higher temperature, and together with peak [1] would again correspond to vanadia without interaction with the sodium ions. For this sample, peak [3] is very narrow ($\Delta T_{1/2}$ = 56 K) and represents *ca.* 58% of the total vanadium loading. This effect is recorded at 846 K and should correspond to reduction of vanadium species strongly interacting with the sodium ions; the Na/(reacted V) ratio is 2.8, and thus this peak can be tentatively ascribed to reduction of Na_3VO_4 species (Na/V = 3).

The behaviour shown by sample V-1 seems to be intermediate between those of sample V-0.5 and sample V-3. Peaks [1] and [2] are again present, although the latter is shifted to higher temperatures (*ca.* 50 K), even more than in sample V-3. These two reduction processes account for *ca.* 38% of the total reduction of V^{5+} to V^{3+}, and since they are also observed in the V-0 sample, they should be ascribed to surface vanadia species with a very slight (or null) interaction with sodium ions. An intense reduction process (peak [3]) is observed at 895 K. If we assume that all vanadium interacting with sodium reduces in this process (508 μmol V/g, 435 μmol Na/g), the Na/V ratio for this species should be 0.85. In such a case, the different values of the Na/V ratio would account for the different positions and full widths at half-height in peak [3] of the TPR profiles of samples V-0.5 and V-1. However, the shift of peak [2] between samples V-0 and V-1 (the largest observed among the samples here reported) could suggest also some interaction of this vanadium species with Na ions, and the Na/V ratio determined for this V-1 sample could be somewhat lower.

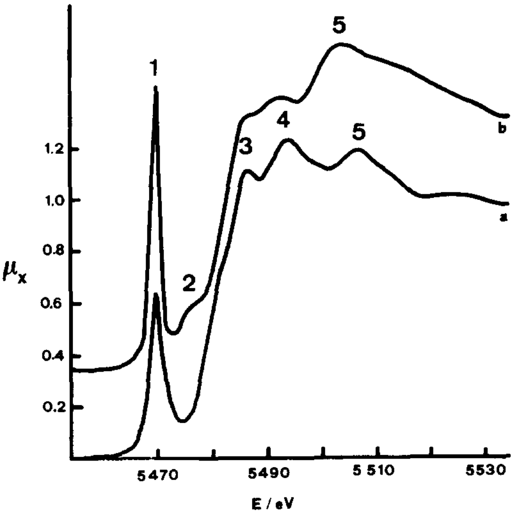

FIG. 7. XANES region of V *K*-edge of (a) V_2O_5 and (b) Na_3VO_4.

XANES

Results described above suggest that in the absence of Na^+ ions, poorly crystallized vanadia is formed on the titania surface. As the sodium content is increased, part of this vanadia interacts with the Na^+ ions, leading to formation of Na_3VO_4 in sample V-3. The XANES spectra of both compounds (V_2O_5 and Na_3VO_4) have been recorded and are shown in Fig. 7. The main difference between these two spectra is in the intensity of the pre-edge peak [1], that is higher for Na_3VO_4 (vanadium in tetrahedral coordination) than for V_2O_5 (vanadium in square pyramidal coordination). This pre-edge peak results from the 1*s*–3*d* transition, that is dipole-forbidden for pure 3*d* orbitals, but

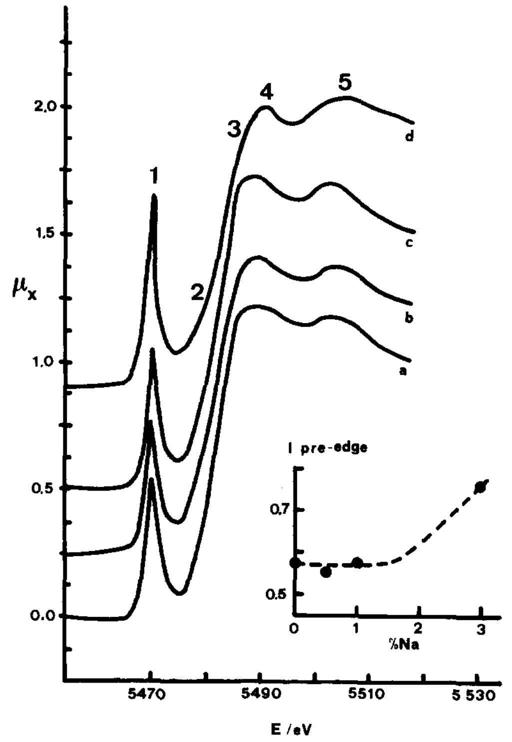

FIG. 8. XANES region of V K-edge of samples (a) V-0, (b) V-0.5, (c) V-1, and (d) V-3. Inset: intensity of the pre-edge peak *vs* Na content (normalized units).

becomes allowed by mixing with oxygen $2p$ orbitals, as in the case of geometries lacking of an inversion center (*28*), and could allow to discern the formation of [VO_4] species. Changes in the positions and relative intensities of the near-edge features [2]–[5] can be also detected between both spectra.

Figure 8 includes the XANES spectra for vanadia–titania samples with 0–3% Na. Up to 1% Na, the spectra are very similar and are unaffected by the presence of sodium, both with regards to the intensity of the first peak, as well as for the shape of the absorption edge. The intensity of the pre-edge feature [1] is nearly constant (Fig. 8, inset) and similar to that recorded for vanadia, while the typical features [2]–[5] appearing after the edge are absent. Actually, spectra for samples V-0 and V-1 are identical to that recorded for highly dispersed vanadia on silica (*27*), where a long-range crystalline structure of vanadia does not exist, although the square pyramidal coordination of vanadium existing in bulk vanadia is maintained. For sample containing 3% Na, the intensity of the pre-edge peak [1] increases appreciably (Fig. 8, inset), although it does not reach the intensity observed for pure Na_3VO_4. It has been previously reported (*29*) that different oxidation states of vanadium would give rise to different electronic occupation of the $3d$ levels, and to changes in the intensity of this pre-edge peak. However, on the basis of our TPR results, a change in the oxidation state of vanadium in the calcined samples upon incorporation of sodium can be discarded, and this increase in the intensity of the pre-edge peak should be better ascribed to a change in the coordination of some of the V^{5+} ions from C_{4v} to T_d. The structure of the absorption edge for this sample also changes, and both the relative intensities of features [4] and [5] and the appearance of shoulders [2] and [3] suggest the presence of Na_3VO_4 in this sample.

CONCLUSIONS

A well-dispersed vanadia–titania system has been prepared, since crystalline V_2O_5 cannot be detected by the experimental techniques here used (XRD, IR or V–UV); XANES indicates that the local coordination around V^{5+} ions is similar to that existing in bulk vanadia (C_{4v}).

When the solid is doped with increasing amounts of sodium up to 3% w/w, two levels of Na–V interaction can be distinguished. For atomic ratios Na/V lower than 0.54 (samples V-0.5 and V-1) new XRD lines are not recorded. However, results obtained by IR and V–UV spectroscopies, as well as by TPR, indicate that an appreciable percentage of vanadia is interacting with sodium ions, thus suggesting the formation of noncrystalline V–Na–O compounds in these samples. From TPR results it can be concluded that the Na/V ratio in these compounds is close to 0.5, and that their formation does not modify the oxidation state of vanadium, which remains as V^{5+}, thus discarding formation of $Na_xV_2O_5$ bronzes previously reported in the literature (5) as the active phase in these systems. XANES shows that at these Na/V ratios the local coordination around the vanadium ions is unaffected by the presence of sodium ions.

A system with a larger Na/V ratio (1.6) has been also characterized, showing a different level of Na–V interaction. New lines are recorded in its XRD profile, but, unfortunately, they cannot be unequivocally ascribed to a single, specific V–Na–O compound. The IR spectra also show new absorptions in the 960–890 cm^{-1} range. Total hydrogen uptake during TPR runs indicate that all vanadium is present as V^{5+} species (bronze formation can be discarded). Deconvolution of the TPR profiles shows that some of the vanadium species remain unaffected by the presence of sodium as poorly crystallized V_2O_5 on the titania surface, in a state fairly similar to that existing in the Na-free sample. In addition, a Na/V atomic ratio close to 3 is calculated for the new V–Na–O compound, thus suggesting formation of some Na_3VO_4. XANES results show that part of the vanadium ions have changed their coordination from square pyramidal to tetrahedral, thus confirming formation of Na_3VO_4.

ACKNOWLEDGMENTS

Financial support from C.I.C.Y.T. (MAT88-556 and PB89-0642) and Consejería de Cultura y Bienestar Social (Junta de Castilla y León) is greatly acknowledged. We express our thanks to the staff of the SRS (Daresbury Laboratories, UK) for their assistance during XAS measurements.

REFERENCES

1. Kung, H. H., *in* "Transition Metal Oxides: Surface Chemistry and Catalysis" (B. Delmon and J. T. Yates, Eds.), p. 1. Elsevier, Amsterdam, 1989.
2. Wainwright, M. S., and Fater, N. R., *Catal. Rev.* **19,** 211 (1979).
3. Haber, J., Kozlowska, A., and Kozlowski, R., *J. Catal.* **102,** 52 (1986).
4. Tanaka, T., Yamashita, H., Tsuchitani, R., Funabiki, T., and Yoshida, S., *J. Chem. Soc., Faraday Trans. 1* **84,** 2987 (1988).
5. Bond, G. C., Sarkany, A. J., and Parfitt, G. D., *J. Catal.* **57,** 476 (1979).
6. Koningsberger, D. C., and Prins, R. (Eds.), "X-ray Absorption: Principles and Applications, Techniques of EXAFS, SEXAFS and XANES". Wiley, New York, 1986.
7. Lytle, F. W., Greegor, R. B., and Raistrick, I. D., *J. Phys., Colloque C8* (*Supl. 12*) **47,** 719 (1986).
8. Bastein, A. G. T. M., van der Bogert, W. J., van der Lee, G., Luo, H., Schuller, B., and Ponec, V., *Appl. Catal.* **29,** 243 (1987).
9. Fransen, T., van Berge, P. C., and Mars, P., *in* "Preparation of Catalysts" (B. Delmon, P. A. Jacobs, and G. Poncelet, Eds.), p. 405. Elsevier, Amsterdam, 1976.
10. Malet, P., and Caballero, A., *J. Chem. Soc. Faraday Trans. 1* **84,** 2369 (1988).
11. "Powder Diffraction File: Inorganic Compounds," International Centre for Diffraction Data, Pennsylvania, 1977.
12. Criado, J. M., and Real, C., *J. Chem. Soc. Faraday Trans 1* **79,** 2765 (1983).
13. Martín, C., and Rives, V., *J. Colloid Interface Sci.* **120,** 469 (1987).
14. Roozeboom, F., Fransen, T., Mars, P., and Gellings, P. J., *Z. Anorg. Allg. Chem.* **449,** 25 (1979).
15. Nakagawa, Y., Ono, T., Miyata, H., and Kubokawa, Y., *J. Chem. Soc. Faraday Trans. 1* **79,** 2929 (1983).
16. Del Arco, M., Hernández, E., Martín, C., and Rives, V., *Spectrosc. Lett.* **22,** 1183 (1989).
17. Borgarello, E., Kiwi, J., Gratzel, M., Pelizzetti, I., and Visca, M., *J. Am. Chem. Soc.* **104,** 2996 (1982).
18. Del Arco, M., Holgado, M. J., Martín, C., and Rives, V., *Mater. Sci. Forum* **25,** 479 (1988).
19. Mateos, J., M. S. Thesis, Universidad de Salamanca, 1988.
20. Del Arco, M., Holgado, M. J., Martín, C., and Rives, V., *Spectrosc. Lett.* **20,** 201 (1987).
21. (a) Jørgensen, C. K., "Absorption Spectra and Chemical Bonding in Complexes." Pergamon Press, Oxford, 1962; (b) Demuynk, J., and Kaufmann, F., *Bull. Soc. Chim. Fr.*, 3840 (1969); (c) Gritsov, A. M., Shuets, V. A., and Kazanskii, U. B., *Kinet. Katal.* **14,** 1062 (1973).
22. Wachs, I. E., Saleh, R. Y., Chan, S. S., and Chersich, C. C., *Appl. Catal.* **15,** 339 (1985).
23. Saley R. Y., Wachs, I. E., Chan, S. S., and Chersich, C. C., *J. Catal.* **98,** 102 (1986).
24. Martin, C., Rives, V., and Gonzalez-Elipe, A. R., *J. Catal.* **114,** 473 (1988).
25. Inomata, M., Mori, K., Miyamoto, T., and Murakami, Y., *J. Phys. Chem.* **87,** 754 (1983).
26. Bond, G. C., Perez Zurita, J., Flamerz, S., Gellings, P. J., Bosch, H., van Ommen, J. G., and Kip, B. J., *Appl. Catal.* **22,** 361 (1986).
27. Muñoz-Paez, A., van Grandelle, J., de Boer, M., van Dillen, A. J., Geus, J. W., and Koningsberger, D. C., *in* "2nd European Conference on Progres in X-ray Synchrotron Radiation Research" (A. Balerna, E. Bernieri, and S. Mobilio, Eds.), p. 555. Soc. Italiana Physica, Bologna, 1990.
28. Wang, J., Lytle, F. W., Messmer, R. P., and Maylotte, D. M., *Phys. Rev. B* **30,** 5596 (1984).
29. Asbrink, S., Greaves, G. N., Haton, P. D., and Garg, K., *J. Appl. Crystallogr.* **19,** 331 (1986).